JTTEE5 11:100-106

TiN-TiB_2 Composite Coatings Reactively Produced by Electrothermally Exploded Powder Spray

Hideki Tamura, Fu-Gao Wei, and Takahiko Kodama

(Submitted 19 September 2000; in revised form 13 November 2000)

Composite coatings composed of titanium nitride, TiN, and diboride, TiB_2, were reactively produced by the electrothermally exploded powder spray technique, in which feedstock powder was prepared from titanium and boron nitride particles. The microstructure of the coating was composed of titanium-ceramic particles the size of which were on the order of several nanometers to a few hundred nanometers. Such reactive thermal spraying brought base-metal saturation into a coating layer at the early stages of coating formation. The ceramic composite spray using feedstock of TiN and TiB_2 particles preferentially brought a new phase of cubic titanium boronitride together with TiN and TiB_2 into a coating. On comparing such a coating to one produced by the conventional method, the reactive thermal spray coating was richer in TiN and TiB_2 due to the excess nitrogen in the feedstock.

Keywords composite coating, electrothermal explosion, metal saturation, reactive thermal spray, titanium boride, titanium nitride

1. Introduction

Some inorganic carbides and nitrides having high melting points, a high degree of hardness, and exhibit good wear resistance. These materials, however, oxidize or decompose, losing carbon or nitrogen into their nonstoichiometric phases under heat treatment. Thus, when thermal spray processing these ceramics, there is the need to suppress such chemical decomposition to maintain their intrinsic properties on metal matrices. When these cermet powders are sprayed, unexpected phases of metal-ceramic composites are produced in the coating, and these exhibit a reduction in the original phases of the feedstock.

The electrothermally exploded powder-spray technique (ELTEPS) can produce coatings of refractory ceramics without any sintering agents and additives to the ceramic feedstocks.[1,2] The feedstock of electric-conductive nonoxide ceramics is Joule-heated by a large electric current and is rapidly sprayed with the high-velocity vapor jet of the feedstock.[3] Therefore, the coating obtained even under depressurized dry-air conditions does not exhibit any major oxide phase.[1,2] The ELTEPS technique, however, has caused decarburization of carbides[2] and has produced nitrogen-deficient titanium nitride.[4]

It has been expected that the amount of element decomposition of the coatings might be decreased by preparing an excess amount of the elements in the feedstock in order to yield titanium mononitride, TiN.[5] When the nitride is produced by chemical reaction during the ELTEPS process, the initial amount of the nitrogen source might be chosen to decrease nitrogen deficiency, x, in a nonstoichiometric phase of TiN_{1-x}. Thus, reactive thermal spraying by this process has undergone trials for producing a TiN-rich coating by using hexagonal boron nitride, h-BN, as the nitrogen source. It has been found that a powder composed of titanium and h-BN particles reacts to produce the composition of titanium nitride and titanium diboride, although no thick coating that is rich in TiN has been characterized in detail yet.

In this article, therefore, the microstructure and composition of such thick coatings are revealed. The reactive thermal spray process and coatings are characterized with reference to composite coatings obtained from a feedstock initially composed of ceramic TiN and TiB_2 particles.

2. Experimental Setup

One of the feedstocks was a mechanically mixed powder of titanium, Ti (Sumitomo Sitix Co., Tokyo, Japan; particle size, less than 150 μm; purity, 99.8%) and hexagonal boron nitride, h-BN (Shin-Etsu Chemical Co., Ltd., Tokyo, Japan; particle size, 10 μm average; purity, 99.7%). Another feedstock was a mixed powder of titanium nitride, TiN (Japan New Metals Co., Ltd., Osaka, Japan; particle size, 1.5 μm average; purity, 99.5%) and titanium diboride, TiB_2 (CERAC, Inc., Milwaukee, WI; particle size, 10 μm average; purity, 99.5%). The mixing was performed in a V-shaped blender for 24 h, with the powder remaining at these initial particle sizes. The molar ratio of Ti to h-BN in the former powder was chosen to allow the following chemical reaction:

$$13Ti + 10BN \rightarrow 8TiN + 5TiB_2 + N_2$$

The molar ratio of TiN to TiB_2 was made to be 8:5 in order to correspond to the production ratio of these composites in the chemical reaction presented above.

Hideki Tamura, Fu-Gao Wei, and **Takahiko Kodama,** Department of Materials Science and Engineering, Tokyo Institute of Technology, Nagatsuta 4259, Midori, Yokohama 226-8502, Japan. Contact e-mail: tamura@materia.titech.ac.jp.

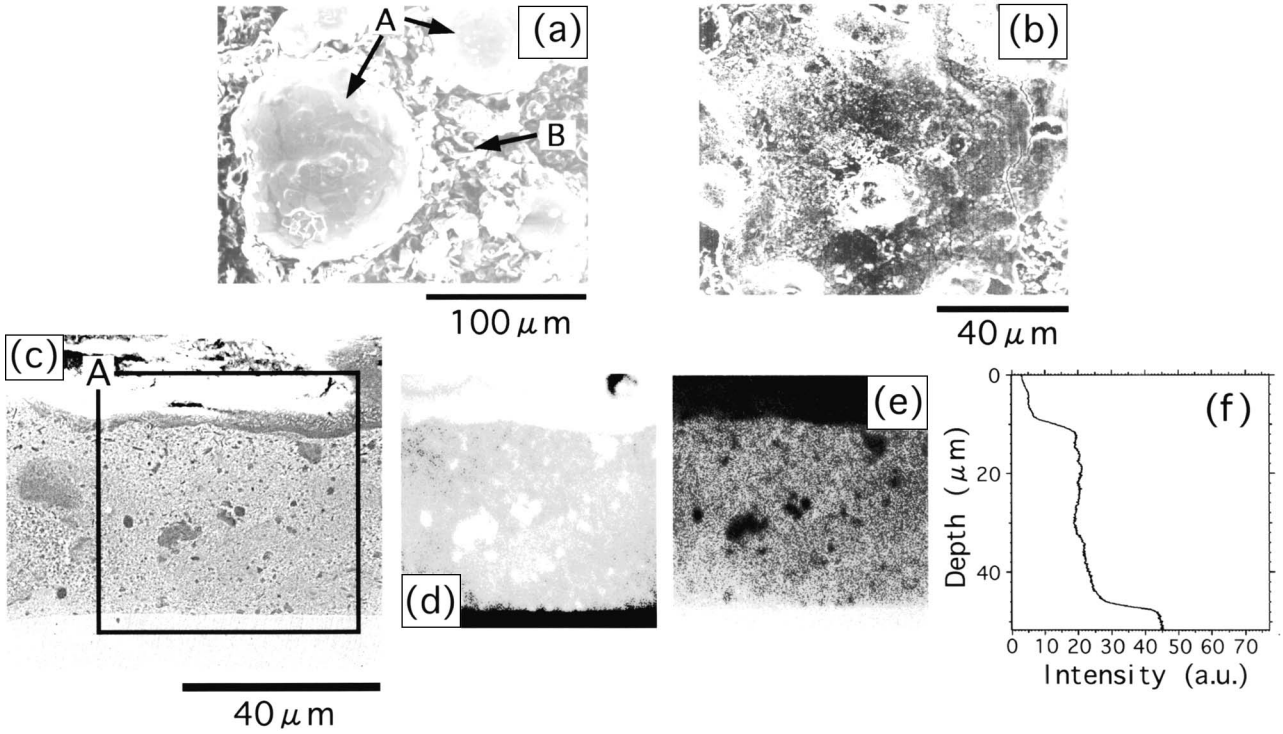

Fig. 1 SEM images of **(a)** starting powder composed of titanium A and boron nitride B, **(b)** the top surface, and **(c)** the cross-section of a coating obtained on a mild-steel substrate by the RTS process. **(d)** Titanium element map on the square area A that was shown in (c). The bright area is rich in the analyzed element. **(e)** An iron element map of the area A shown in (c). **(f)** The depth profile of iron accumulated over the map of (e).

Each feedstock was charged into a specially designed container at a relative density of ~59% under argon gas of atmospheric pressure. The container was concentrically composed of an inner polyethylene tube and an outer cylindrical metal jacket that had a window for the ejection of the tube contents.[3] The container was sealed at both ends with a pair of tungsten electrodes. In order to guide a spray jet coming from the window, a plastic nozzle was installed in the container.[6] The container was placed in a spray chamber and was held by a pair of electrical contacts connected to a high-voltage circuit having a large-capacity condenser.[5]

Twenty-five substrates of mild steel, each of which had a mirror-polished top surface of 10 × 10 mm^2, were fixed on a plate holder that faced the window of the powder container at a standoff distance of 80 mm. The spray chamber was filled with nitrogen at 6.7×10^3 Pa prior to spraying. A maximum voltage of 8.3 kV was applied to the powder for its electrical breakdown. The joule heat arising in the powder was estimated from the time-varying voltage and current applied to the powder.[1] Micromorphology and constituent elements of the obtained coatings were characterized with a scanning electron microscope (SEM, JEOL Co. model JSM-5310, Tokyo, Japan) and an electron probe microanalyzer (EPMA model EPMA-1400, Shimazu Co., Tokyo, Japan), respectively. A field-emission-type SEM (FE-SEM Hitachi Co. model S-4500, Tokyo, Japan) and a transmission electron microscope (TEM, JEOL Co. model JEM-2011) were used for structural characterization. The constitutive crystal phases of the coatings were identified with an x-ray diffraction (XRD) analyzer (Mac Science model M18XHF, Tokyo, Japan) using CuK_α radiation. The Vickers microhardness of the coatings was measured with a hardness tester (Akashi Co. model MVK-EIII, Tokyo, Japan). Ten indents were made to find a hardness of an area in the coatings.

3. Experimental Results and Discussion

3.1 Reactive Thermal Spray Coating with Base-Metal Saturation

A joule heat (i.e., specific energy) of 10.6 MJ/kg was supplied to a Ti-BN powder of 7.3×10^{-4} kg for approximate 60 μs until the beginning of spray jetting. Figure 1 shows the SEM images of the starting powder, a coating surface obtained on a substrate, and its cross-section. The surface does not exhibit any of the initial features of the feedstock particles. It was formed through the successive deposition of molten materials and solidification. The cross-section, which was polished after resin molding and cutting of the coating, shows no pores and cracks under the top surface of the coating. The XRD analysis was applied to the feedstock and the surface, as is shown in Fig. 2(a) and (b), respectively. It is clear that the titanium and boron nitride reacted to form the different composites. The diffraction peaks from these phases correspond to those of titanium diboride, TiB_2, titanium nitride, TiN, and an unknown phase of cubic crystal structure, as is discussed further in section 3.5. Thus, the

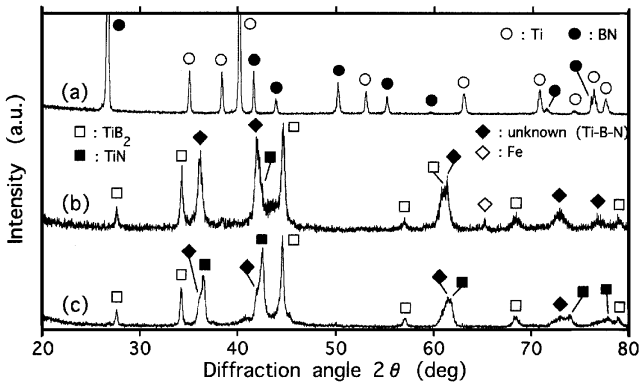

Fig. 2 XRD pattern of **(a)** the starting powder composed of titanium and boron nitride, **(b)** the coating surface obtained on a mild-steel substrate by a single process of the RTS, and **(c)** the coating surface obtained by a twofold RTS.

coating consisted of the deposition of such boride and nitride produced under the reactive thermal spray of the ELTEPS process.

The element detection by electron probe microanalysis (EPMA) was performed on the cross-section, and this is shown in Fig. 1(d) and (e) for the mapping of titanium and iron, respectively. The bright areas are rich in these detected elements. According to the XRD analysis above, the titanium detection indicates the existence of titanium boride, nitride, and boronitride. Thus, Fig. 1(d) shows the distribution of the titanium-bearing phases to a depth of approximate 40 μm from the top surface.

The iron detection shown in Fig. 1(e) indicates a wide distribution from the bottom (i.e., the base substrate) to a depth of several micrometers under the coating surface. The depth profile of the iron viewed in Fig. 1(e) is shown in Fig. 1(f), where it is observed that the iron is virtually homogeneously distributed over a depth of approximately 35 μm. Only the top area of several micrometers in depth is very rich in the titanium composites. Thus, the coating is characterized with the deposition of the titanium composites of reaction products, which was saturated almost up to the top surface by the base metal. Such base metal saturation has been obtained in other coatings.[1,2,4,5] It has been found also that the enhancement of spray-jet flow is effective in producing such saturation.[6] In fact, the depth profile obtained here shows a deeper and more homogeneous distribution of the base metal than that reported in Ref. 5, since the spray conducted here was focused onto substrates by the nozzle in contrast to the previous one, which did not employ a nozzle.

The Vickers microhardness of this metal-saturated layer ranged from 14 to 15 GPa, when the load and loading time was 50g and 10 s. Since the titanium composites are mixed with the base metal, which has a hardness of 1.5 GPa, its hardness is smaller than those of bulk TiB_2 and TiN (34 and 21 GPa, respectively).[7]

3.2 Thick Composite Coating by Reactive Thermal Spray Process

In order to form a thick layer that is rich in ceramics on a substrate, a twofold spray process was conducted. The coating obtained is shown in Fig. 3. The first and second spray procedures were carried out at specific energies of 11.2 MJ/kg and 8.6 MJ/kg, respectively. The top surface of the coating is shown in Fig. 3(a), and it was formed through the successive deposition of molten droplets. Its cross-sections (Fig. 3b and c) reveal a layer of approximately 80 to 90 μm in thickness. The crystal structure of the coating top surface was analyzed by XRD (Fig. 2c). The diffraction peaks correspond to those of TiB_2, TiN, and an unknown phase of cubic titanium boronitride, which also could be included in the single-coated specimen shown in Fig. 1. The diffraction peaks of cubic TiN are more distinct than those in the single coating and are comparable to those of TiB_2. The diffraction peak of iron that appears at the angle 2 θ of approximate 65° in Fig. 2(b) does not appear in Fig. 2(c). Thus, this twofold-sprayed coating is richer in the titanium composites and has a larger volume fraction of TiN than the single coating. The constituents of the twofold coating were observed by EPMA and are shown in Fig. 3(d) and (e). The coating layer was richer in titanium composites than in iron. This is found more clearly in Fig. 3(f) (i.e., the depth profile of the iron accumulated over the area marked in Fig. 3e). Therefore, a thick ceramic layer was obtained.

The Vickers microhardness of the layer was measured in two areas (i.e., the upper and lower halves of the layer) and ranged from 20 to 24 GPa and from 24 to 26 GPa, respectively. The lower half contained less iron than the upper portion and, as shown in Fig. 3(d), was harder. Thus, the thick layer was richer in titanium compounds than the single coating and was also harder.

Figures 3(g) and (h) show the highly magnified images of the typical microstructures of the upper and lower halves of the layer, respectively. The area of existing iron is shown in bright contrast, whereas the ceramic-dominant area appears dark. It is shown in Fig. 3(g) that each domain of the ceramic and iron is shaped irregularly and that its representative size is a few micrometers at most. Figure 3(h) shows very fine regions of ceramic and iron that are difficult to distinguish. These are submicrometers in size and are much smaller than the feedstock particles. Figure 3(i) shows a magnified image of an area of drastic change in the iron distribution that was shown in Fig. 3(f). According to the depth profile, the iron density decreases within a 5 μm depth from the substrate into the layer. It is observed that the iron disperses into the layer and decreases its domain size.

3.3 Nanometer-Sized Particle Composite by Reactive Thermal Spray Process

In order to identify the microstructure and crystal phase of the ceramic layer of titanium composites, TEM was conducted on a coating that was sprayed by the twofold method. A small disk for the TEM analysis was prepared by mechanical thinning of the substrate parallel to its top surface, and the disk thickness was reduced to approximate 100 μm. The center of the disk was thinned on both sides of the disk by argon-ion milling at 5 kV and finally was perforated within the ceramic layer. Figure 4(a) shows a typical bright-field image of the specimen, and Fig. 4(b), (c), and (d) show the diffraction patterns of the selected area corresponding to the local areas labeled by A, B, and C, respectively, in Fig. 4(a). The broad diffraction rings shown in Fig. 4(b) are characteristic of an amorphous structure in area A.

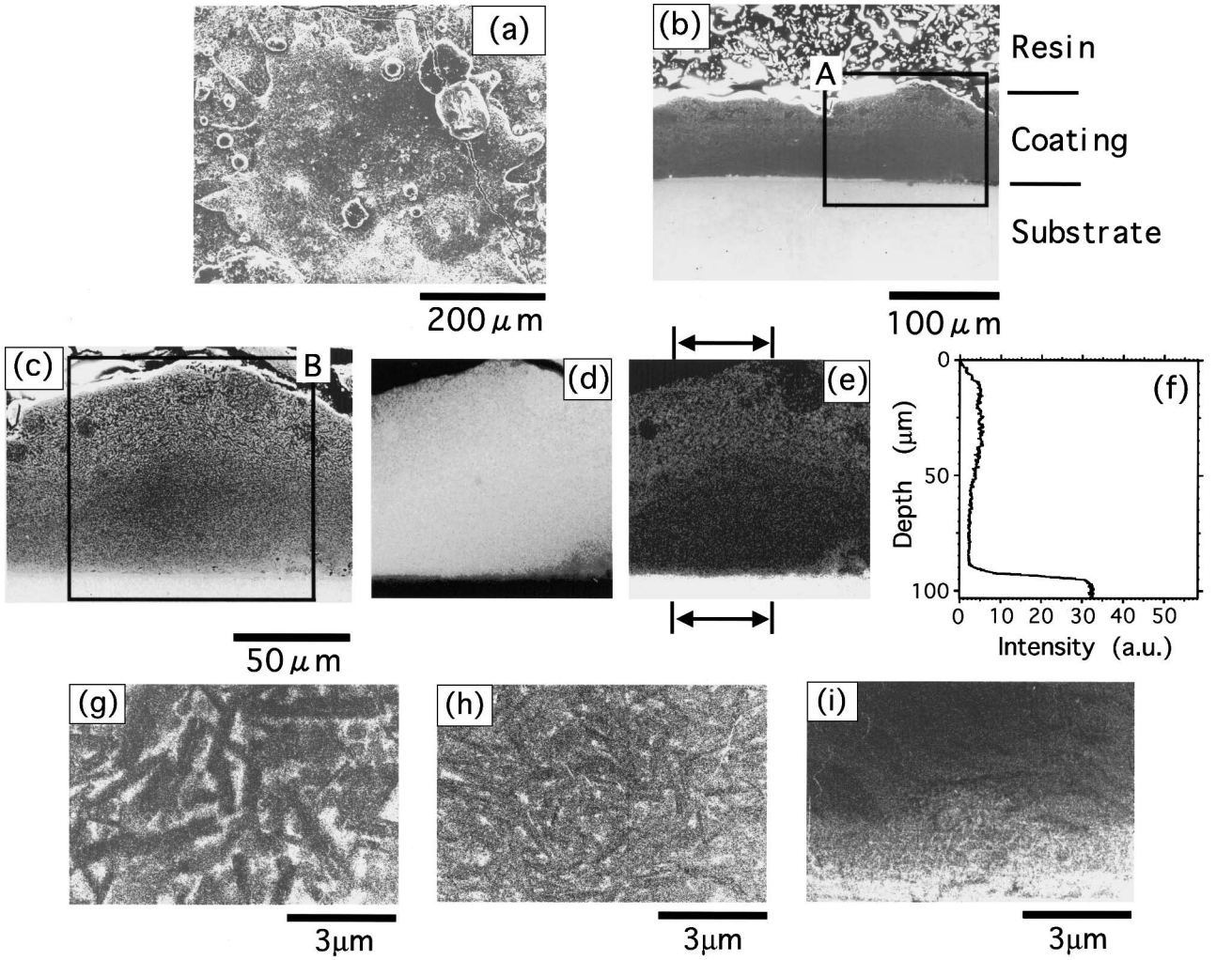

Fig. 3 SEM images of **(a)** the top surface, **(b)** the cross-section of a coating obtained on a mild-steel substrate by a twofold RTS, and **(c)** the magnification of area A in (b). **(d)** A titanium element map of the area B shown in (c). The bright area is rich in the analyzed element. **(e)** An iron element map of the area A shown in (c). **(f)** The depth profile of iron accumulated over the marked area shown in (e). Highly magnified SEM images of typical structures of **(g)** the upper and **(h)** the lower halves of the coating cross-section. **(i)** A magnified image of a typical area including the drastic change of the iron profile shown in (f).

The diffraction pattern taken from area B shows sharp rings and strongly indicates the presence of very fine crystalline phases. In combination with the dark-field observation, such phases were of sizes on the order of a nanometer. The diffraction patterns from area C can be overlaid on the same rings obtained for area B, but they are not continuous due to the coarsening of the crystalline phases. These phases remain fine, on the order of tens of nanometers in size.

A high cooling rate during the solidification of the sprayed ceramic layer is considered to be responsible for the formation of such amorphous and nanometer-sized phases. The microstructure shown in Fig. 4(a) corresponds to the initial stage of the rapid solidification process in which much undercooling suppresses the nucleation of the crystallization or the growth of nuclei. However, a smaller amount of undercooling accompanying the continuing solidification results in a coarser microstructure. Such coarser structure is shown in Fig. 4(e), which is taken from an area close to that of Fig. 4(a). Here the particles that can be found are on the order of tens of nanometers to a few hundred nanometers. Diffraction of the selected area by using a large selected-area aperture also shows a pattern of rings that is similar to those from areas B and C in Fig. 4(a). As shown in Fig. 4(f), the indexed rings are made of TiN and TiB_2. Dark-field images of relatively coarse particles were observed with the confirmation of diffraction spots of TiB_2 and TiN (not shown here), then particles of both TiB_2 and TiN were identified to be a granular shape, with irregular boundaries and almost equal size. Thus, it is difficult to differentiate them from each other only by bright-field observation. Apart from the TiN and TiB_2 phases, a new phase formed in the TiN and TiB_2 matrices, taking a needle-like shape (Fig. 4e). The new phase was determined by electron-beam-diffraction analysis to be of a hexagonal structure with a = 2.94 Å and c = 21.98 Å. This is explained as a long-period ordered structure of TiB_2 (a = 3.0303 Å; c = 3.2295 Å) along the c axis due to stacking faults with a period that is about seven times at large as that of TiB_2.

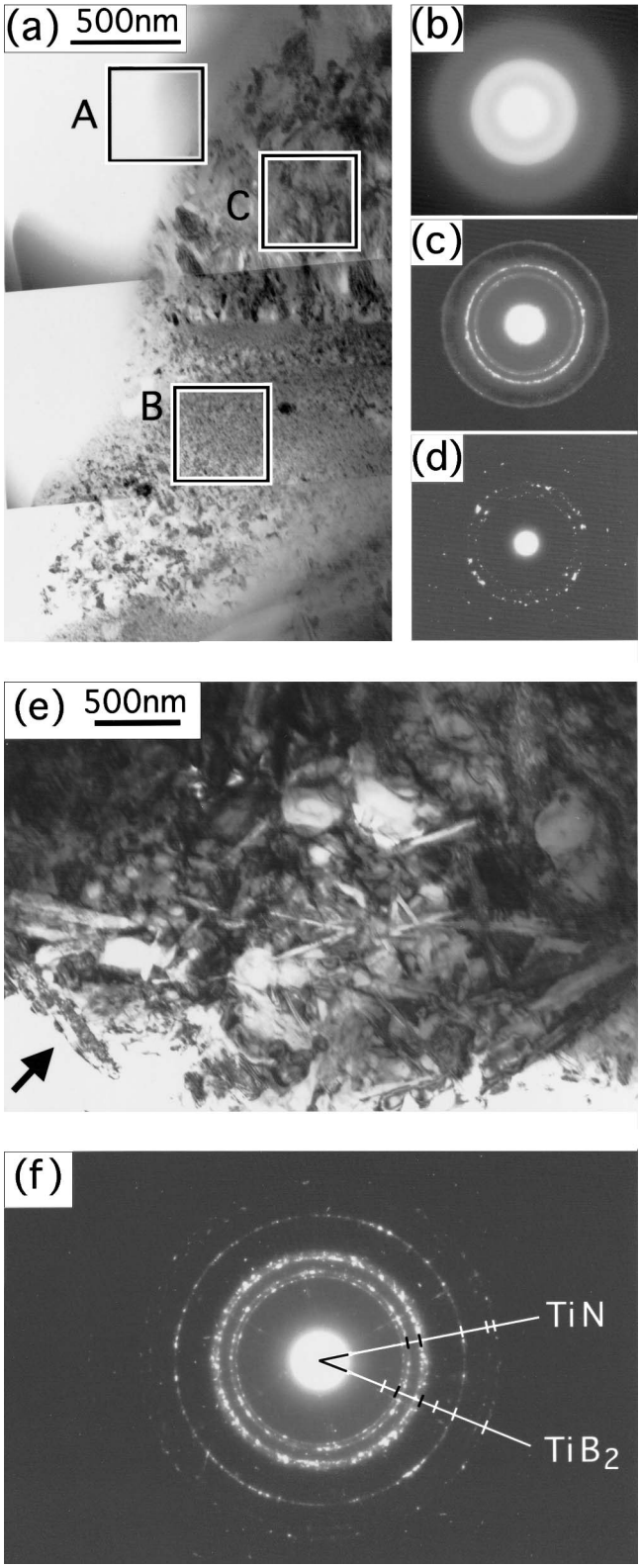

Fig. 4 **(a)** A typical bright-field image of titanium-composite ceramics. Selected-area diffraction patterns of the local areas labeled by **(b)** A, **(c)** B, and **(d)** C shown in (a). **(e)** A bright-field image of relatively coarse microstructure in a area close to that shown in (a). **(f)** Selected-area diffraction rings obtained from the area shown in (e). The rings are indexed to be TiN and TiB_2.

3.4 Micrometer-Sized Particle Composite by Ceramic-Composite Spray Process

The reactive thermal spray (RTS) process described in the above sections is compared to another process in which a feedstock consisting of TiN and TiB_2 particles was heated by a specific energy of 12.2 MJ/kg. This energy corresponds to 2.8 times the theoretical energy of 4.3 MJ/kg that is necessary to melt the feedstock when using the specific heats[8] and heats of fusion[9] of TiN and TiB_2. As described in section 3.1, the specific energy supplied to the Ti-BN powder for the single coating was 10.6 MJ/kg and was less than that in the ceramic-composite spray (CCS) process. However, the energy of 10.6 MJ/kg in the RTS process corresponds effectively to 12.5 MJ/kg when based on the total enthalpy of the chemical products of $8TiN + 5TiB_2 + N_2$. That is because the total enthalpy of the starting system of 13Ti + 10BN is 1.9 MJ/kg larger than that of the chemical products. Thus, the specific energy supplied to the feedstock in this CCS process is comparable to the effective specific energy in the RTS process.

Figure 5 shows the typical SEM images of the feedstock particles, the coating top surface, and its cross-section. The surface does not exhibit any of the initial features of the feedstock and shows the successive deposition of molten materials and solidification. The cross-section shows well-contrasted domains ranging from a few micrometers to 10 μm in size. This contrast arose from the roughness of the sectioned surface and should result from preferential breaks at relatively weak boundaries of the domains. The Vickers microhardness of this coating ranged from 24 to 28 GPa when the load and loading time were 50g and 10 s, respectively. This hardness is comparable to those of well-sintered TiB_2 and TiN.[7]

Figure 6(b) shows the existence of TiB_2, TiN, and an unknown titanium-boronitride phase, while Fig. 6(a) shows only TiB_2 and TiN phases in the feedstock. The largest diffraction peak of TiN appears at 2 θ of 42.6° in Fig. 6(a), and it is comparable to that of TiB_2 at 2 θ of 44.4°. For the coating, however, the TiN peak decreased in comparison to that of TiB_2, as shown in Fig. 6(b), while the unknown peaks appeared through the decomposition of the feedstock.

The element maps were made by EPMA, as shown in Fig. 5(d) and (e). The depth profile of iron distribution viewed in Fig. 5(e) is shown in Fig. 5(f). Only the local penetration of iron is seen in Fig. 5(e), ranging from a few micrometers to 10 μm in depth. However, since there is no large-scale saturation of the base metal into the coating, the coating is composed only of titanium composites with a thickness of about 70 μm. The structure of this coating is quite different from that of the RTS coating shown in Fig. 1(c), even with almost the same specific energy. The difference between the microstructures needs to be discussed in terms of detailed physics. The size, impact velocity, deposition rate, temperature of the spraying droplets, and the mutual relationship of the feedstocks and the substrate materials are not identified here.

Another difference is found in the phase content. Chemical decomposition in the CCS process made the diffraction peaks of the unknown phase larger than those of TiN, as shown in Fig. 6(b). On the contrary, the second coating formed from the RTS process realized a ceramic-rich layer and made the diffraction peaks of TiN larger than those of the unknown, as shown in Fig.

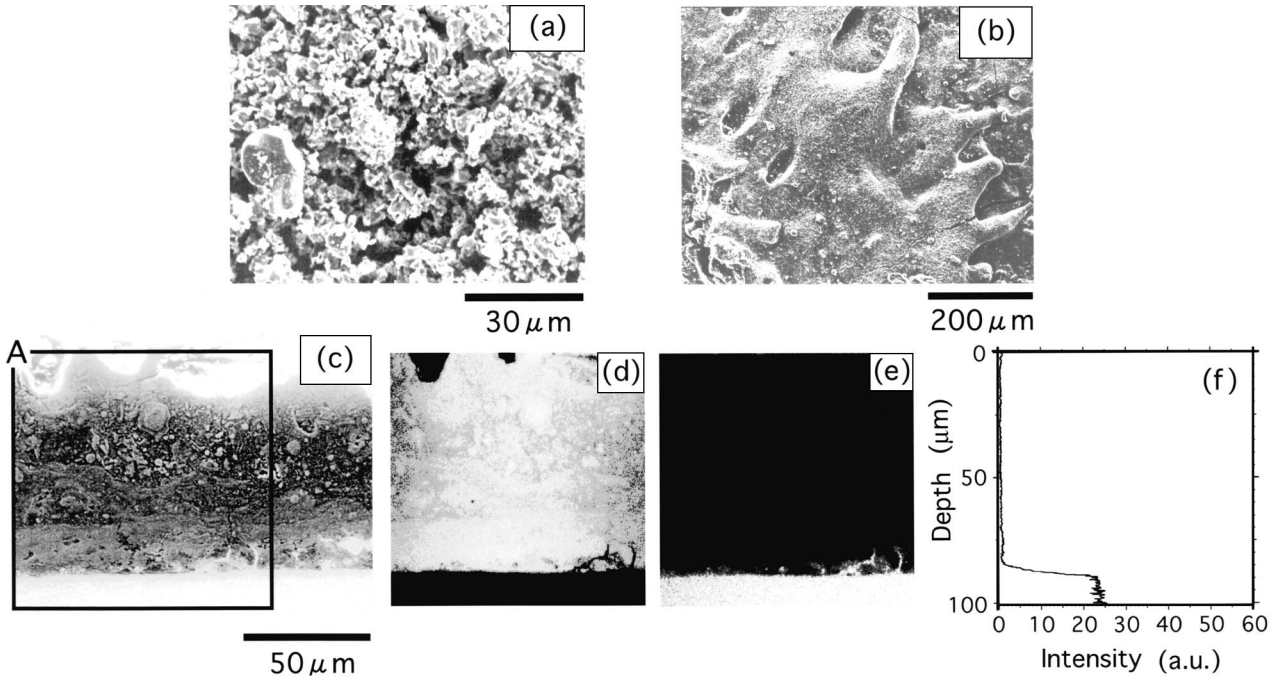

Fig. 5 SEM images of **(a)** starting powder composed of titanium nitride and titanium diboride, **(b)** the top surface, and **(c)** the cross-section of a coating obtained on a mild-steel substrate by the CCS. **(d)** A titanium element map of the area A shown in (c). The bright area is rich in the analyzed element. (e) An iron element map of the area A shown in (c). **(f)** The depth profile of iron accumulated over the map of (e).

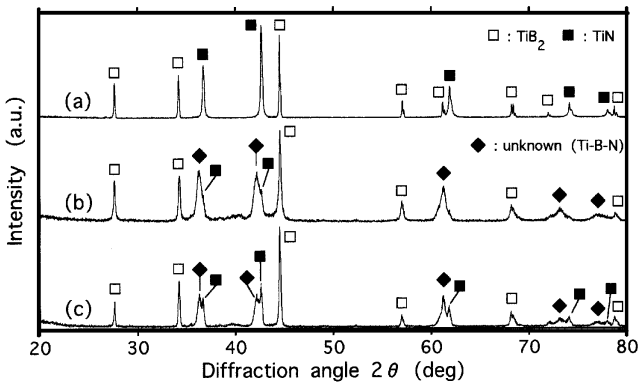

Fig. 6 XRD patterns of **(a)** starting powder composed of titanium nitride and titanium diboride, **(b)** the coating surface obtained on a mild-steel substrate by the CCS with a specific energy of 12.2 MJ/kg, and **(c)** the coating surface obtained with a specific energy of 7.5 MJ/kg.

2(c). The coating was formed with the specific energy of 8.6 MJ/kg. Its effective energy corresponds to 10.5 MJ/kg when added to the enthalpy difference of 1.9 MJ/kg on the basis of the reaction products. The energy of 12.2 MJ/kg in this CCS process is larger than the 10.5 MJ/kg. This excess energy might enhance the decomposition of the feedstock. Thus, a much lower energy of 7.5 MJ/kg was supplied to a feedstock under another CCS test, and the XRD pattern from the coating surface obtained is shown in Fig. 6(c). Although the constituent phases are the same as those of the highly energized coating, the peaks of the unknown phase are still larger or comparable to those of TiN. Even a low amount of energy can cause a significant amount of decomposition of the feedstock in the CCS.

3.5 Decomposition of TiN Yielding New Phase and Its Suppression

The ELTEPS process[4] has sprayed the feedstocks composed only of TiB_2 or TiN, and it has been found that the constituent phase of the coatings is only TiB_2 or TiN_{1-x}. Thus, the ELTEPS process brings about the apparent decomposition of TiN in its coating, not in the TiB_2 coating. It also has become known that titanium nitride of TiN_{1-x} in the cubic phase of a NaCl-type structure has a wide range of possible nitrogen deficiencies, x, due to its nonstoichiometry,[10] and that its lattice parameter depends on the deficiency of a well-defined relationship.[10] The authors have found in separate experiments using XRD analysis that the nitrogen deficiency of TiN coatings increases with a specific energy supplied to a TiN feedstock, for example, $x = 0.13$ and 0.35 for specific energies of 11.0 and 17.8 MJ/kg, respectively. In the present CCS experiments, therefore, the significant amount of nitrogen deficiency that is detectable also must arise from its composite feedstock underspraying.

Although some amount of such nitrogen-deficient TiN_{1-x} should exist separately from TiN and TiB_2 in a coating, further deficiency might form cubic titanium boronitrides (TiN_yB_z with $y + Z > 1$) together with borides. It has been found that their lattice parameters are 4.25 and 4.23 Å for $TiN_{0.78}B_{0.42}$ and $TiN_{0.77}B_{0.54}$, respectively.[11] These should be formed by an interstitial solid solution, because of the total number of atoms per unit cell was larger than eight. It also has been noticed that boron atoms can replace nitrogen atoms in TiN_{1-x} in large amounts without a change of structure despite the large differences in their atomic radii.[11] The unknown phase in the present work corresponds to a cubic phase with a lattice parameter of 4.27 Å when based on its diffraction angles and the lattice strain of other

known phases. This parameter is a little larger than the 4.24 Å of TiN, TiN_{1-x}, and TiN_yB_z with $y + z < 1$, and it is closer to the 4.25 Å of $TiN_{0.78}B_{0.42}$. In addition, the diffraction peaks of the unknown phase increase with the decrease of the peaks of TiN and/or TiN_{1-x}, more than that of the TiB_2 peaks. This fact is suggestive of the possible production of a new phase of $4TiN_yB_z$ with $y + z > 1$ from TiB_2 and $3TiN_{1-x}$ for $x < 1/3$.

In the RTS process, molecular nitrogen of 0.84×10^{-3} mol would be prepared in the feedstock as one of the ideal reaction products of $8TiN + 5TiB_2 + N_2$. This amount corresponds to the molecular nitrogen gas of 99×10^5 Pa at 293 K in the powder container. This gas must achieve its higher pressure through heating and decomposition in the container. This pressure is estimated to be much larger than nitrogen-vapor pressure even at the melting point of TiN.[7] Thus, the nitrogen excessively surrounding TiN particles should have a chance to enter the particle surfaces and to suppress the nitrogen deficiency of TiN. Such suppression would decrease the production of the titanium boronitrides. In fact, the RTS process makes the ceramic layer richer in the TiN phase than does the CCS process, comparing Fig. 2(c) to Fig. 6(b) and (c).

4. Conclusions

The composite coating of titanium nitride and boride was reactively produced from the feedstock powder of titanium and boron nitride by the electrothermally exploded powder spray technique. The homogeneous saturation of base metal was obtained in the coating layer by an enhanced ceramic jet directed with a nozzle. The twofold spray method produced a ceramic layer that was rich in titanium composites. The layer exhibited no pores and cracks, and revealed a microhardness that was comparable to those of well-sintered titanium ceramics. The layer was composed of crystalline particles of titanium nitride and titanium diboride, which were on the order of a nanometer to a few hundred nanometers in size.

The feedstock powder of titanium nitride and diboride was used to form a CCS. A ceramic layer rich in titanium composites was produced with the element diffusion only around the boundary of the layer and substrate, where its specific energy of Joule heat was comparable to that of the RTS process. The layer was composed of domains on the order of a few micrometers to 10 μm in size without pores, and its microhardness attained that of titanium ceramics. An unknown cubic phase of titanium boronitride was obtained preferentially in the coatings that were formed via the CCS process. The amount of the phase increased with the specific energy supplied to the feedstock. It was thought that the phase should be produced through the solid solution of titanium boride with partially decomposed titanium nitride. In the RTS process, however, in which an excess amount of nitrogen had been prepared in the feedstock, the unknown titanium boronitride was not obtained to the same extent, while the amount of titanium nitride was greater. The RTS process, therefore, effectively suppressed the decomposition of titanium nitride and was capable of controlling the coating composition.

Acknowledgments

This work was supported by Grant in Aid for Exploratory Research No. 09875175 of the Ministry of Education, Science, Sports and Culture in Japan. The authors thank Japan New Metals Co., Ltd., Sumitomo Sitix Co., and Shin-Etsu Chemical Co., Ltd., for supplying titanium nitride, titanium, and boron nitride, respectively.

References

1. H. Tamura, M. Konoue, and A.B. Sawaoka: "Zirconium Boride and Tantalum Carbide Coatings Sprayed by Electrothermal Explosion of Powders," *J. Thermal Spray Technol.,* 1997, *6,* pp. 463-68.
2. T. Soda, H. Tamura, and A.B. Sawaoka: "Refractory Carbide Coatings Sprayed by Electrothermal Explosion of Conductive-Ceramic Powders," in *Thermal Spray: Meeting the Challenges of the 21st Century,* C. Coddet, ed., ASM International, Materials Park, OH, 1998, *2,* pp. 1351-56.
3. H. Tamura, M. Konoue, Y. Ikeda, T. Soda, and A.B. Sawaoka: "Generation of a High-Velocity Jet in the Electrothermal Explosion of Conductive Ceramic Powders," *J. Thermal Spray Technol.,* 1998, *7,* pp. 87-92.
4. Y. Ikeda, H. Tamura, and A.B. Sawaoka: "Refractory Boride and Nitride Ceramic Coatings Sprayed by Ceramic Jets," *Rev. High Pressure Sci. Technol.,* 1998, *7,* pp. 1472-74.
5. T. Kodama, Y. Ikeda, and H. Tamura: "Reactive Thermal Spray by High Velocity Ceramic Jet and Characterization of the Coatings," *J. Thermal Spray Technol.,* 1999, *8,* pp. 537-44.
6. H. Tamura and M. Itaya: "Base-Metal Saturation of Refractory Carbide Coatings Produced by Enhanced Ceramic Jets in Electrothermally Exploded Powder Spray," *J. Thermal Spray Technol.,* 2000, *9,* pp. 389-93.
7. G.V. Samsonov and I.M. Vinitskii, ed.: *Handbook of Refractory Compounds,* IFI/Plenum, New York, 1980, pp. 183, 292, 295.
8. Y.S. Touloukian, ed.: *Thermophysical Properties of High Temperature Solid Materials,* Macmillan Company, New York, 1967, *5,* p. 575; *6,* p. 240.
9. J.A. Dean, ed.: *Lange's Handbook of Chemistry,* McGraw-Hill, New York, 1979, p. 132.
10. H.A. Wreidt and J.M. Murray: *Bull. Alloy Phase Diagrams,* 1987, *8,* p. 378.
11. S.I. Alymovskii, Yu.G. Zainulin, G.P. Shveikin, P.V. Gel'd, and N.V. Bausova: "Lattice Defects in the Cubic (NaCl-type) Boronitride of Zirconium and Titanium," *Inorganic Mater.,* 1975, *11,* pp. 148-49.